scientific reports

OPEN

Identification of a disulfidptosis-related genes signature for diagnostic and immune infiltration characteristics in endometriosis

Xiangyu Chang & Jinwei Miao✉

Endometriosis (EMs) is the prevalent gynecological disease with the typical features of intricate pathogenesis and immune-related factors. Currently, there is no effective therapeutic intervention for EMs. Disulfidptosis, the cell death pattern discovered recently, may show close relationships to immunity and EMs. In this study, bioinformatics analysis was used to investigate the role of disulfide breakdown related genes (DRGs) in EMs. The EMs gene expression matrix was subjected to differential analysis for identifying overlap between differentially expressed genes (DEGs) in EMs and genes associated with disulfide poisoning. Immunoinfiltration analysis was performed. In addition, the association of hub genes with immune cells was examined. Multiple machine learning methods were employed to identify hub genes, construction of predictive models, and validation using external datasets and clinical samples. Totally 15 overlapping genes were identified. Immune-correlation analysis showed that NK cells played a vital role, and these 15 genes were closely related to NK cells. PDLIM1 was further determined as the hub gene through machine learning techniques. Clinical samples and external datasets were adopted for validating the performance in diagnosis. According to the above findings, we built the predictive model, and calculated the AUCs obtained from three external validation datasets to demonstrate the model accuracy. RT-qPCR and IHC analyses were applied to confirm the results. Colony formation was used to verify the effect of PDLIM1 on the proliferation of primary EMs cells. A strong correlation between disulfidptosis and EMs was identified in this study, highlighting its close correlation with the immune microenvironment. Moreover, our results shed new lights on exploring biomarkers and potential therapeutic targets for EMs.

Keywords Endometriosis, Disulfidptosis, Biomarkers, Immune

Endometriosis (EMs) is the prevalent gynecological disease, commonly occurring in 10-15% of reproductive-age females[1,2]. EMs gives rise to dysmenorrhea or chronic pelvic pain and infertility, significantly affecting women's health and overall quality of life. Characterized by extensive and diverse lesions, EMs exhibits an extremely invasive and recurrent nature, usually referred to as both a "benign cancer" and a "refractory disease". Surgical treatment is still the diagnostic gold standard. However, EMs has been currently identified as the systemic condition not restricted to pelvic diseases only[3]. Recently, EMs has been identified to be closely associated with autoimmunity and inflammation[4,5].

In recent years, with advancements in immunology research, significant changes have been observed in humoral and cellular immune functions among EM patients[6-8]. Due to its unknown pathogenic mechanism, non-specific symptoms, and absence of non-invasive indicators for detection, EMs is usually not diagnosed in a timely manner. Therefore, it is crucial to explore the mechanism and early diagnosis of EMs. Various cell death patterns, including pyroptosis, apoptosis, cuproptosis or ferroptosis during EMs are widely explored to discover markers that can be used to predict prognosis and treat EMs[9-11]. Regulated cell death (RCD) provides a vital idea to make the investigation.

In March 2023[12], disulfide molecules accumulate at a large amount in glucose-deficient SLC7A11-high cancer cells, which causes aberrant disulfide bonding among actin cytoskeleton proteins, and interference with the tissue, finally resulting in actin network breakdown or even the novel cell death pattern known as disulfidptosis.

Department of Gynecologic Oncology, Beijing Obstetrics and Gynecology Hospital, Capital Medical University, Beijing Maternal and Child Health Care Hospital, No. 251, Yaojiayuan Road, Chaoyang District, Beijing, China. ✉email: jinweimiao@ccmu.edu.cn

nature portfolio

The significance of SLC7A11 and glucose metabolism in the pathogenesis and progression of EMs has been demonstrated by a number of studies[13,14]. Thus, disulfidptosis may be related to EMs, even though more studies are needed to explore the underlying mechanism.

Gene Expression Omnibus (GEO) database was used to investigate the possible mechanisms of EMs by examining differentially expressed genes (DEGs) in EMs compared with healthy samples. Cross-referencing analysis was also performed in DEGs with disultioptose-related genes (DRGs), aiming to identify differential DRGs and evaluate their correlation with immune cells. Then, diverse machine learning methods were employed to identify hub genes and construct predictive models. Later, the modal map and two external datasets were used to validate model performance, providing novel insights into understanding molecular mechanisms associated with EMs pathogenic mechanism.

Materials and methods
Data source
Four raw datasets (GSE7305[15], GSE23339[16], GSE6364[17], and GSE51981[18]) were obtained from the GEO database. GSE51981 included 77 EMs samples and 34 normal controls (without other common uterine/pelvic pathologies). GSE6364 included 21 EMs and 16 normal control samples, whereas GSE7305 involved 10 EMs and 10 normal control samples. GSE23339 dataset contains endometrial samples from 9 individual women and 10 EMs samples. The "remove Batch Effect" function was used to eliminate batch effects with R package "limma". In addition, "normalize Between Arrays" function was applied in data standardization. Figure 1 shows the flowchart of analysis.

### Detection of DEGs related to EMs and disulfidptosis
Differential analysis was performed with R package "limma"[19]. DEGs were screened in EMs compared with healthy samples upon thresholds of Log2| FoldChange | (Log|FC|) < 1 or > 1, and $P < 0.05$. Then, heatmaps and volcano plots were drawn to show differential gene expression. Gene ontology (GO) and Kyoto Encyclopedia of Genes and Genomes (KEGG) enrichment was conducted using R package "clusterProfiler"[20] to explore gene biological functions. Based on Liu et al.[12,21], 31 DRGs were obtained. Afterwards, DEGs (GSE7305, $P < 0.05$) were crossed with DRGs to acquire 15 differentially expressed DRGs.

Analysis of infiltrating immune cells
The 22 kinds of lymphocytes were analyzed for their levels in EC and EU samples using CIBERSORT algorithm and immune cell LM22 gene set[22]. Immune cell infiltrating levels were analyzed according to expression matrix of every sample[23]. GSEA was applied in single-sample gene set enrichment analysis (ssGSEA)[24]. Spearman correlation was performed to visualize the correlation of these 15 genes. The association of immune infiltration with DRGs was analyzed with R packages dplyr, stringr, ggpubr, ggplot2, igraph, ggraph, corrr, corrplot, tidyverse, and reshape2[25].

Construction of predictive model by machine learning
In this study, five machine learning approaches were used for screening candidate diagnostic genes of EMs. As a regression approach, least absolute shrinkage and selection operator (LASSO) contributes to improving
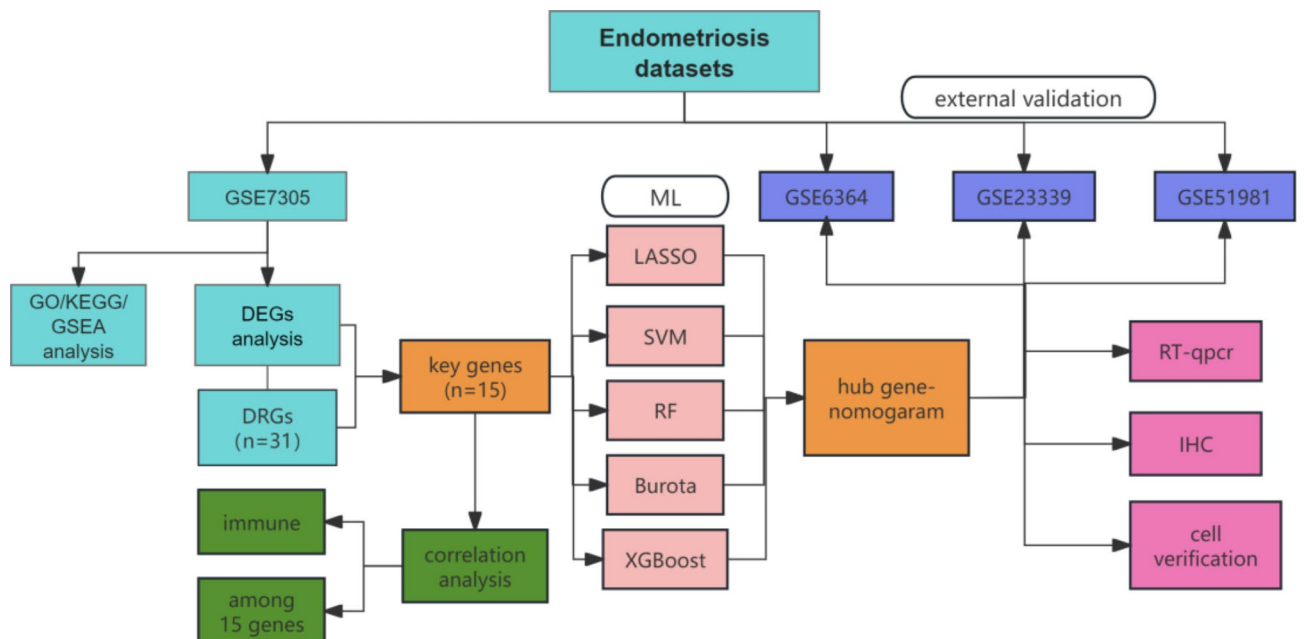
Fig. 1. The study flow chart.

prediction performance and selecting key variables with regularization technologies[26]. SVM has been developed as the classification or regression supervised machine learning approach, requiring a training set with labels (16). SVM-RFE is another machine learning method that trains features of diverse categories for shrinking feature set and finding the most significant features[27]. Random forest (RF) is an excellent method to provide stable prediction and predict continuous variables[27]. Machine learning technique Boruta is used for feature selection to screen out every feature set associated with dependent variables[28]. The XGBoost prediction model can be used to further improve the model prediction performance[29]. Genes intersected among LASSO regression, SVM, RF, Boruta and XGBoost prediction model analyses were considered as central diagnostic hub genes of EMs. The R version was 4.2.3, and the main package version glmnet involved was 4.1.8.

Construction and validation of a nomogram for EMs diagnosis

Subsequently, 'RMS' package (version 6.2-0) used to create the biomarker-based nomogram, aiming to help evaluate EMs occurrence. Then, calibration curves were drawn to evaluate the nomogram prediction accuracy. ROC analysis was conducted using three external datasets GSE23339, GSE6364, GSE51981 to demonstrating the significance of our prediction model in diagnosing the disease in EMs relative to normal groups.

Real-time PCR analysis

Using TRIzol reagent, total RNAs in EMs and normal control tissues were extracted in line with specific protocols. Then, RNA 1 mg, HifairIII 1st Strand SuperMix (YEASEN,11137ES60) and Hieff qPCR SYBR Green Master Mix (YEASEN,11201ES60) were adopted for reverse transcription. This reaction was found in Bio-Rad CFX96 PCR System. The 2-11Ct method was adopted for data normalization, and β-actin served as the endogenous control. Primers who were adopted for recognizing bisulfite-modified regions (-6 to -290) in PDLIM1 promoter included 5′-GTAGAGTTGTTGAGAGTTTTGG-3′ (forward, F), 5′-AATCTATCTACTAAATAATCATAACAC-3′ (reverse, R); β-actin: 5′-CCCTGGAGAAGAGCTACGAG-3′ (F), 5′-GGAAGGAAGGCTGGAAGAGT-3′ (R).

IHC analysis

Tissue samples were obtained during laparoscopic operations and washed by PBS to remove blood and impurities, followed by rapid freezing and storage. Afterwards, to prepare tissue blocks, 4% paraformaldehyde was added to fix the sample prior to paraffin embedding. Then, the sections were incubated with primary antibody PDLIM1/CLP36 Polyclonal antibody (11674-1-AP,1:500) overnight under 4 ℃. After being incubated for another one hour, using Dako REAL EnVision Detection System (K5007; Dako, Jena, Germany), sections were washed by PBS, and treated with DAB + chromogen buffer (K5007, Dako) to visualize immunostaining. After counterstaining, images were obtained under the optical microscope (Nikon, DS-U3).

Isolation and culture of primary endometrial cells and endometriosis cells

The ectopic lesion tissues of endometriosis patients were taken, and the blood and mucus on the tissues were washed with PBS according to the method described in previous study[30], and then cut into small pieces ina sterile petri dish (1 mm3). 0.3% collagenase IV was added to the tissue pieces (Solarbio, Beijing, China). Digest at 37℃ for 20 min. Equal-volume complete medium DMEM/F12 (Procell, Wuhan, China) was added to collect cell suspension and terminate enzyme digestion. Cell suspensions were filtered through 100 μm cell filter (Corning, New York, NY, USA), cell suspensions were centrifuged to collect cell precipitates, and cells were cultured at a temperature of 37 °C, a CO2 concentration of 5%, and a humidity level of 95%, under conditions using DMEM/F12 medium.

Cell transfection

SiRNA was synthesized by Beijing Syngentech Co., LTD. Transfection procedures were performed using Lipofectamine 3000 (Invitrogen, USA), as per manufacturer's instructions. The target sequence is as follows: Si-PDLIM1-1 target sequence: GTCATCACAAACCAGTACA, Si-PDLIM1-2: AGGAGAAGCAAGAGTTAAA and Si-PDLIM1-3: GTGGCATCAACCTGAAACA.

Colony formation

In the colony formation assay, EMs stromal cells were inoculated in a 6-well plate at a density of 1×10^3 cells/well. The plates were then incubated at 37 °C and 5% CO2 for 14 days. The colonies were fixed with 4% paraformaldehyde and stained with 0.1% crystal violet. Count the number of colonies in each well, each containing more than 50 cells. The experiment was repeated three times.

Statistical analysis

Data were expressed as mean standard deviation (SD). Bioinformatics analyses were performed with R software (v.4.2.3). GraphPad Prism analysis software was used in statistical analysis. $P < 0.05$ represented statistical significance.

Results

DEGs detection and functional and pathway analysis

Four GEO datasets were obtained for analysis. One analysis was showed(GSE7305). Volcano Plots and heatmaps were drawn to display DEGs (Fig. 2A,B). GO and KEGG analyses were carried out with to investigate DEGs functions. The important GO-BP (biological process) terms were mostly associated with the development of urogenital system, protein zinc ion homeostasia, protein nitrosytation, organelle fission and so on. Based on GO-CC (cell component) enrichment, DEGs of the four datasets were significantly associated with cell
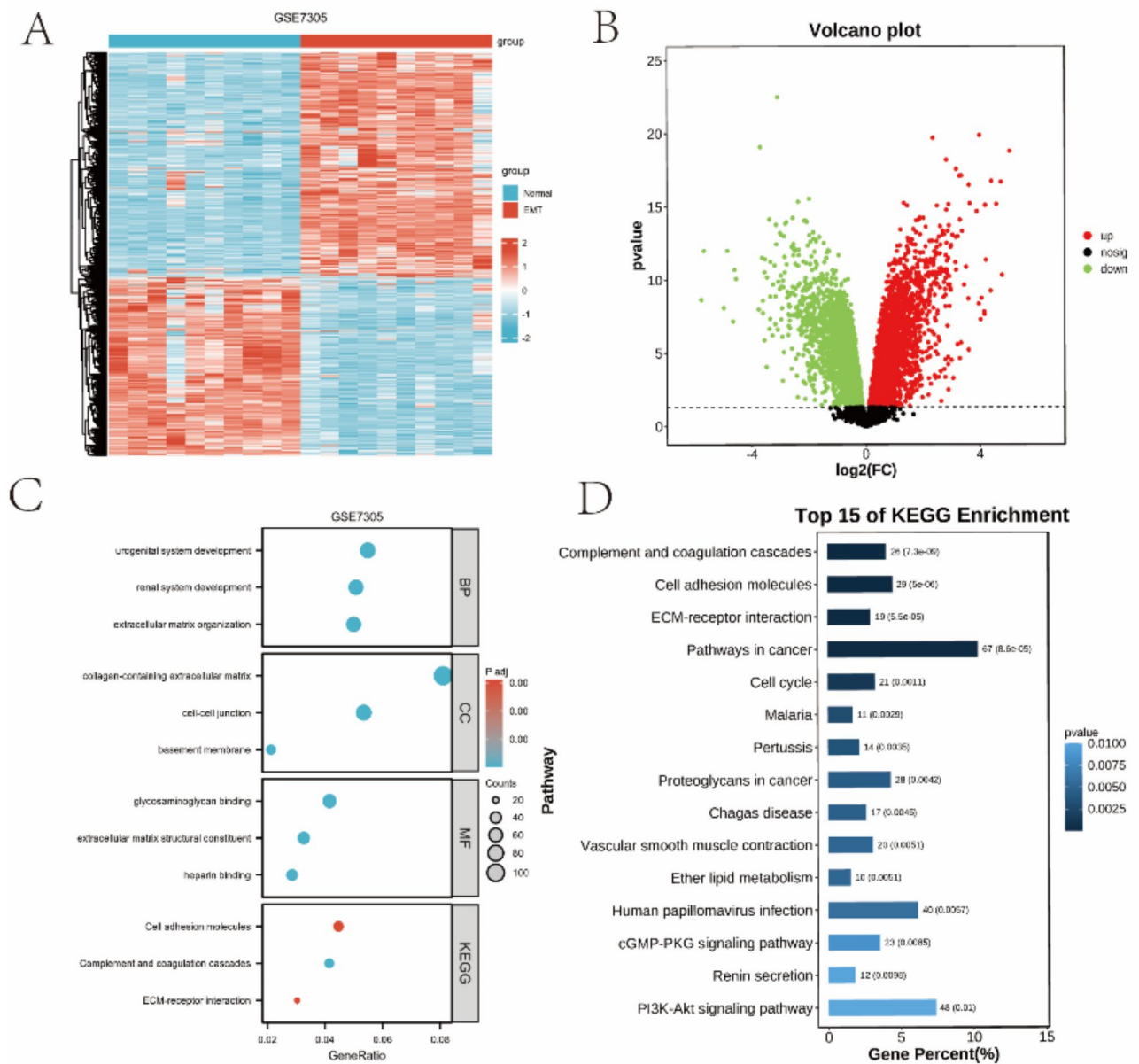
Fig. 2. DEG detection. (**A**) Heatmap displays the expression levels of EMs-related DEGs in GSE7305. (**B**) volcano plot showing significant DEGs of GSE7305. (**C**) GO annotation displays enriched terms associated with EMs. (**D**) KEGG analysis suggests pathways enriched into EMs. *GO* gene ontology, *BP* biological process, *CC* cellular component, *MF* molecular function, *KEGG* Kyoto Encyclopedia of Genes and Genomes.

junctions, basement membrane, collagen-containing extracellular matrix and spindle. DEGs were significantly related to GO-MF (molecular function) terms including Glycosaminoglycan binding, immune receptor activity, extracellular matrix structural constituent, and transcription coactivator activity (GSE7305 was showed in Fig. 2C). Using KEGG enrichment, these DEGs of four datasets were associated with Cell cycle, Cell adhesion molecules, Glutathione metabolism, IL-17 pathway, Human T-cell leukemia virus 1 infection, Human T-cell leukemia virus 1 infection, Estrogen signaling pathway, Cytokine-cytokine receptor interaction, Inflammatory bowel disease, Cholesterol metabolism, actin binding and so on (GSE7305 was showed in Fig. 2D). The findings indicate that disulfidptosis is closely related to Glutathione metabolism, immune response, and inflammatory factors, suggesting the significant role of disulfidptosis in EMs.

Immune functional pathways detected by GSEA

Gene Set Enrichment Analysis (GSEA) was carried out using C5.bp.v7.4.symbols.gmt reference gene set in order to explore mechanisms involved in EMs pathogenic mechanism(Fig. 3). Differences between individuals with EMs and normal controls were of significance, particularly in terms of B cell receptor pathway, B cell-mediated immunity, leukocyte mediated immunity, and humoral immune response. Notably, there was a significantly
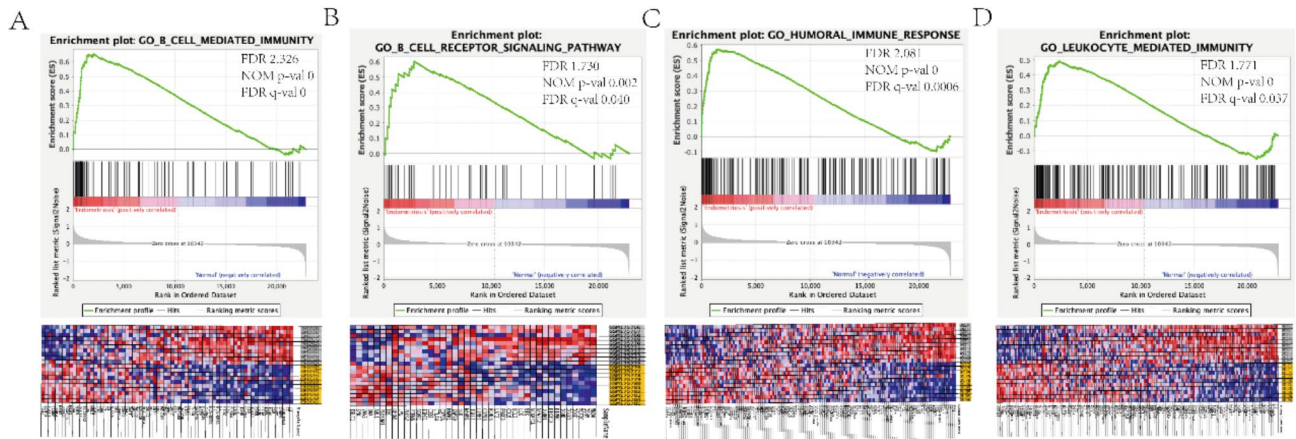
Fig. 3. GSEA on pathways in EMs and normal groups (GSE7305).

enhanced humoral immune response in individuals with EMs, which was shown to be closely associated with B-cell-related immunity.

Analysis of infiltrating immune cells

For the 31 DRGs, their expression profiles in EMs versus healthy samples were analyzed. There were altogether 15 hub genes obtained through the intersection of 102,231 DEGs with 31 DRGs (Fig. 4A), including OXSM, MYH10, RAC1, RPN1, IQGAP1, CD2AP, PDLIM1, GYS1, ACTN4, FLNB, TLN1, PSMD2, CYFIP1, WASF2, and ABI2.

To evaluate immune infiltration levels among EMs patients, the CIBERSORT algorithm was employed to analyze immune cell percentages in EMs. Immune cell maps and correlation maps were drawn for 22 immune cell types (Fig. 4D,F) in EMs samples. Therefore, EMs patients showed significantly decreased abundances of activated NK cells, T cells CD8, T cells follicular helper, T cells regulatory (Tregs), and NK cells resting; while increased abundances of B cells naïve, plasma cells, Macrophages M2, and T cells CD4 memory resting (Fig. 4E).

### The association of DRGs with immune infiltration in EMs

Among 15 differentially expressed DRGs (Fig. 4A) in EMs, IQGAP1, ACTN4, FLNB, TLN1, and WASF2 exhibited significant overexpression. In addition, ABI2 was significantly overexpressed, while OXSM, MYH10, RAC1, RPN1, CD2AP, PDLIM1 and GYS1 were significantly down-regulated. PSMD2 and CYFIP1 were up-regulated in normal samples. Heatmaps and grouping box maps (Fig. 4B,C) were used to visualize the expression patterns of these 15 genes. Clearly, among these key genes, OXSM showed a significant negative association with ABI2 but positive correlations with PSMD2, GYS1, and RPN1; MYH10 was negatively related to IQGAP1; RAC1 was negatively correlated with ABI2; while RPN1 demonstrated positive correlations with CYFIP1, PSMD2, GYS1, and PDLIM1. PDLIM1 showed a positively correlation with CYFIP1, whereas PSMD2 showed a positive correlation with GYS1. ACTN4 displayed a negative correlation with CYFIP1. In terms of immune cell analysis for the correlations of these 15 key genes, NK cells exhibited strong associations, indicating that unique immune cell infiltration in EMs was probably closely associated with disulfidptosis, while DRGs were likely to be vital for the regulation of immune microenvironment in EMs (Fig. 4A,G,H).

Machine learning-based disulfidptosis-signature identification

Based on LASSO regression, random forest, SVM-REF, Boruta, and XGBoost algorithms based on 15 key genes, this study identified candidate genes and constructed the disulfidptosis-signature (Fig. 5A–D). The standard error λ of the minimum distance in the Lasso regression model was determined to be 0.065. TLN1, CYFIP1, PDLIM1, RPN1, and IQGAP1 were selected as significant variables in this model. The use of the SVM-REFCV method for feature selection yielded two factors, IQGAP1 and PDLIM1. By adopting the Burota method for confirmation purposes, GYS1, FLNB, TLN1, CYFIP1, PSMD2, WASF2, ABI2, PDLIM1, CD2AP, IQGAP1, RPN1 and OXSM were found to be relevant genes. Variable importance analysis using XGBoost revealed that PDLIM1 had the highest importance score; while Random Forest Regressor indicated that five variables with the highest significance included PDLIM1, RPN1, PSMD2, CYFIP1, and GYS1. Finally, the intersection of these five machine learning algorithms obtained PDLIM1 as the hub gene for the construction of our model (Fig. 5E).

Hub gene level validated by differential analysis with external datasets

The nomogram model was prepared to diagnose EMs. The calibration curve demonstrated minimal error between actual and predicted risks, indicating excellent prediction accuracy of the nomogram model (Fig. 6A,B). External datasets GSE23339, GSE6364, and GSE51981 were utilized for further validation purposes, demonstrating the diagnostic value of hub genes with area under the curve (AUC) values being 0.889 for GSE23339, 0.773 for GSE51981, and 0.631 for GSE6364 (Fig. 6C–E). The obtained findings highlight the substantial diagnostic
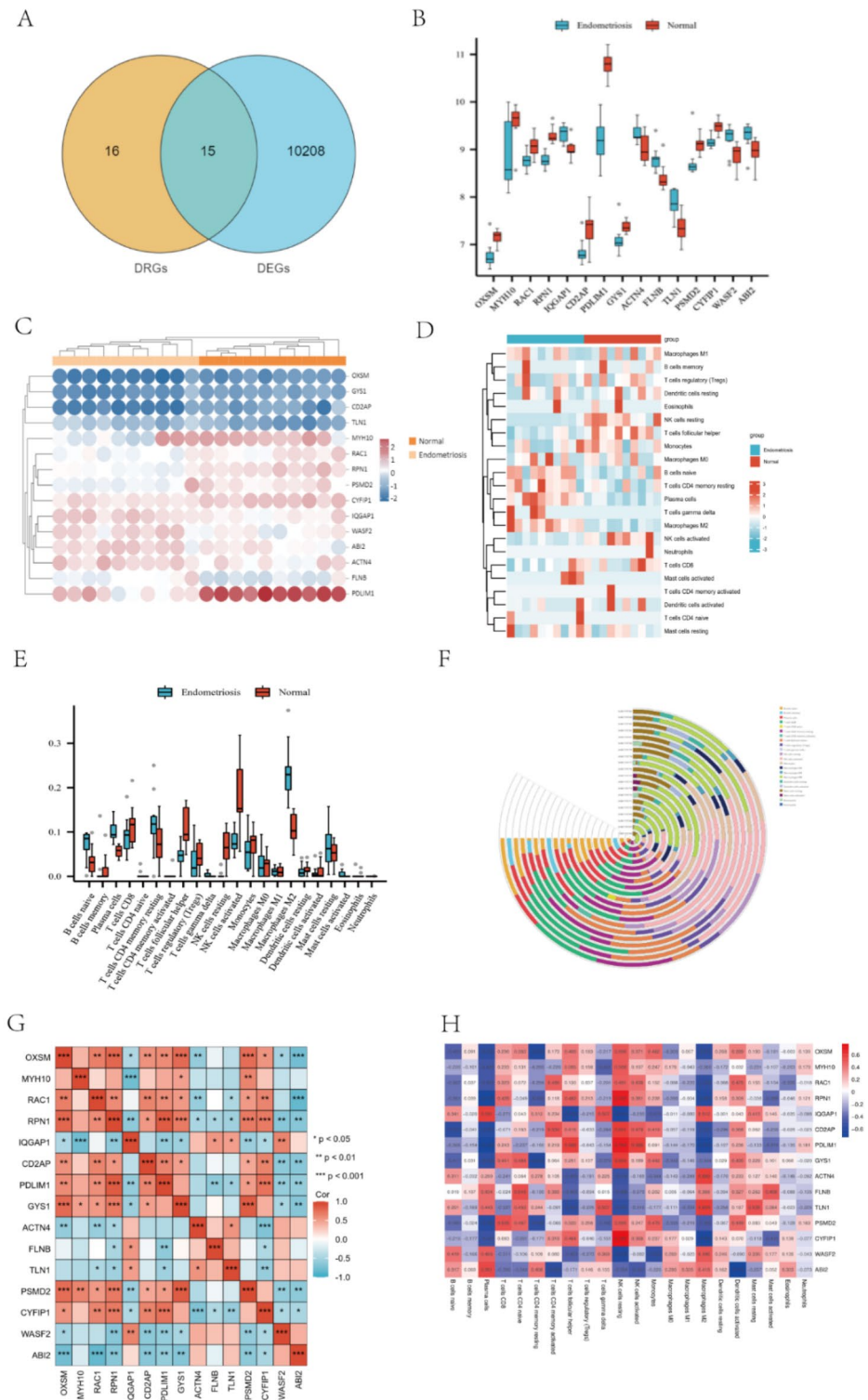
Fig. 4. DRGs levels and immune cell infiltrating degrees within EMs. (**A**) Overlap of genes between DEGs and DRGs. (**B**) Boxplot showing DRGs expression profiles. (**C**) Heatmap displaying DRGs expression. (**D**) Heatmap representing percentages of 22 infiltrating immune cells within EMs and healthy controls. (**E**) Boxplots exhibiting diverse immune infiltration degrees in EMs compared with normal samples. (**F**) Infiltrating immune cell percentages within EMs and healthy samples were compared. (**G**) Correlation analysis of 15 key genes. (**H**) Correlation analysis of 15 key genes and infiltrated immune cells.
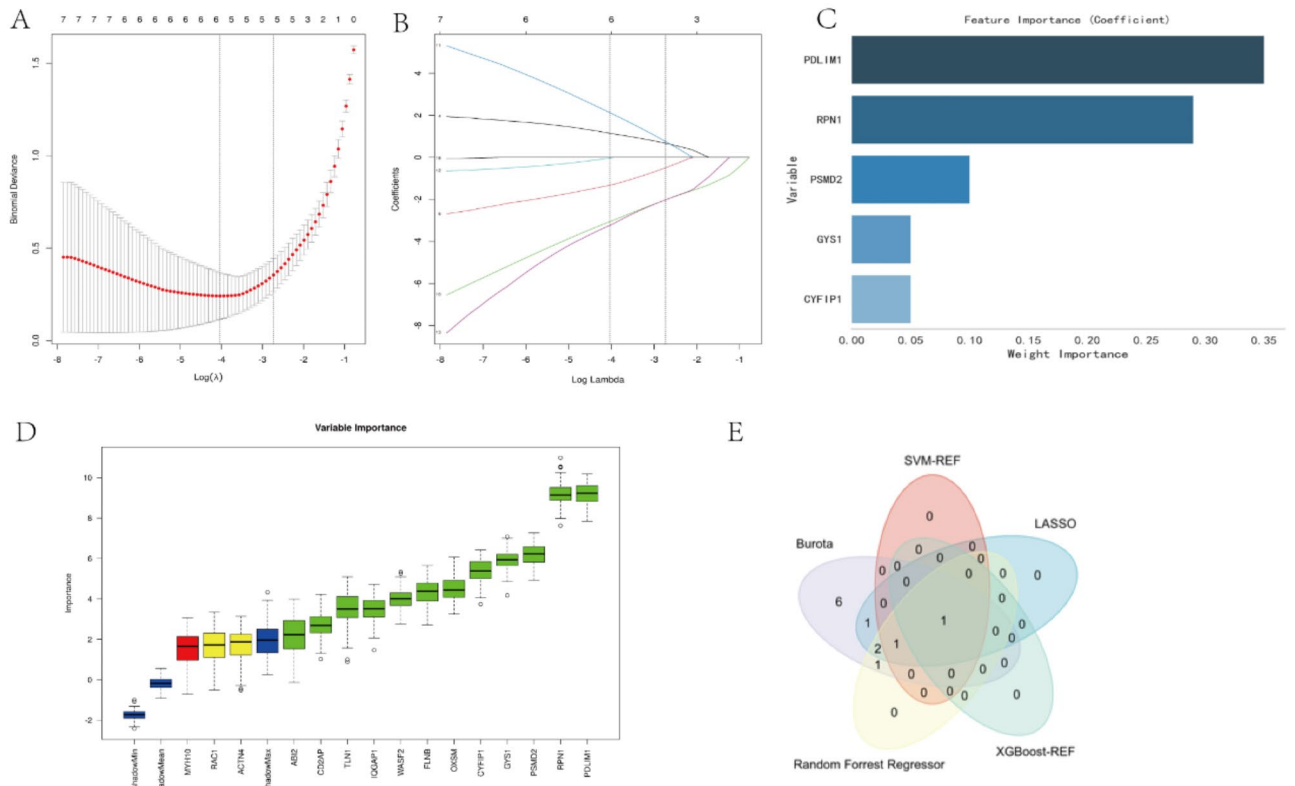
Fig. 5. Disulfidptosis-signature construction based on machine learning. (**A,B**) LASSO algorithm adopted for the construction of disulfidptosis-signatures. (**C**) RF algorithm applied in ranking genes according to their importance. (**D**) The Burota algorithm. Tentative is yellow, Rejected is red, Accepted is green, and Shadow is blue. (**E**) Venn diagram displaying overlap of possible genes obtained from five algorithms.

significance of nomogram model and suggest that the gene can effectively distinguish between EMs and normal groups.

Validation of PDLIM1 level by real-time PCR and IHC

To validate reliability of our hub gene, samples were obtained from EMs patients ($n=3$) and normal human endometrium ($n=3$) to conduct qRT-PCR and IHC. As a result, PDLIM1 expression was significantly reduced in EMs at mRNA and protein levels (Fig. 7A,B). Subsequently, we evaluated the effect of down-regulation of PDLIM1 on the proliferation of primary EMs cells by the colony formation assay. We found that cell proliferation decreased after PDLIM1 knockdown compared to the control group. (Fig. 7C)

Discussion

EMs, a benign disease, lacks effective markers and therapeutic drugs, posing significant challenges for women of childbearing age. The theory of retrograde menstruation put forward in 1921 by Sampson has been extensively studied and widely accepted as an explanation. In addition, alternative hypotheses including vascular/lymphatic metastasis and coelomic metaplasia are released for elucidating the EMs pathophysiology[31]. However, no single hypothesis comprehensively accounts for all pathological types. Furthermore, immune, genetic, endocrine, and environmental factors have been suggested to be related to the EMs pathogenesis.

Disulfidptosis, which has been recently identified as the new cell death pattern, can be induced by disulfide bond accumulation. This results in the cytoskeleton collapse and later cellular demise, exhibiting a close association with disease progression[32]. PCD mechanisms, including apoptosis, necorsis or autophagy, is important for the modulation of disease progression and immune microenvironment. Pharmacological agents for inducing specific cell death pathways have demonstrated effectiveness in tumor treatment. While research on ferroptosis has reached significant maturity[33], more attention needs to be paid to disulfidoptosis as a new cell death mode. Disulfidptosis is induced by redox imbalance related to glucose and amino acid metabolic disturbance. These two metabolisms play vital roles in biological processes including immune evasion, metastasis, or drug resistance[34,35]. Disulfidptosis, as the novel PCD form, is potentially correlated with tumor immune response. The precise mechanism underlying disulfidptosis and the regulation of diverse disorders, along with candidate pathways, need to be further explored. Since the emergence of disulfidptosis in 2023, studies have been carried out to explore the intricate associations between hepatocellular carcinoma, pancreatic cancer, Alzheimer's disease, and disulfidptosis[36-38]. The pathogenesis of disulfidptosis and EMs has been linked for the first time in this study. Candidate hub genes and targets are explored through bioinformatics analysis.
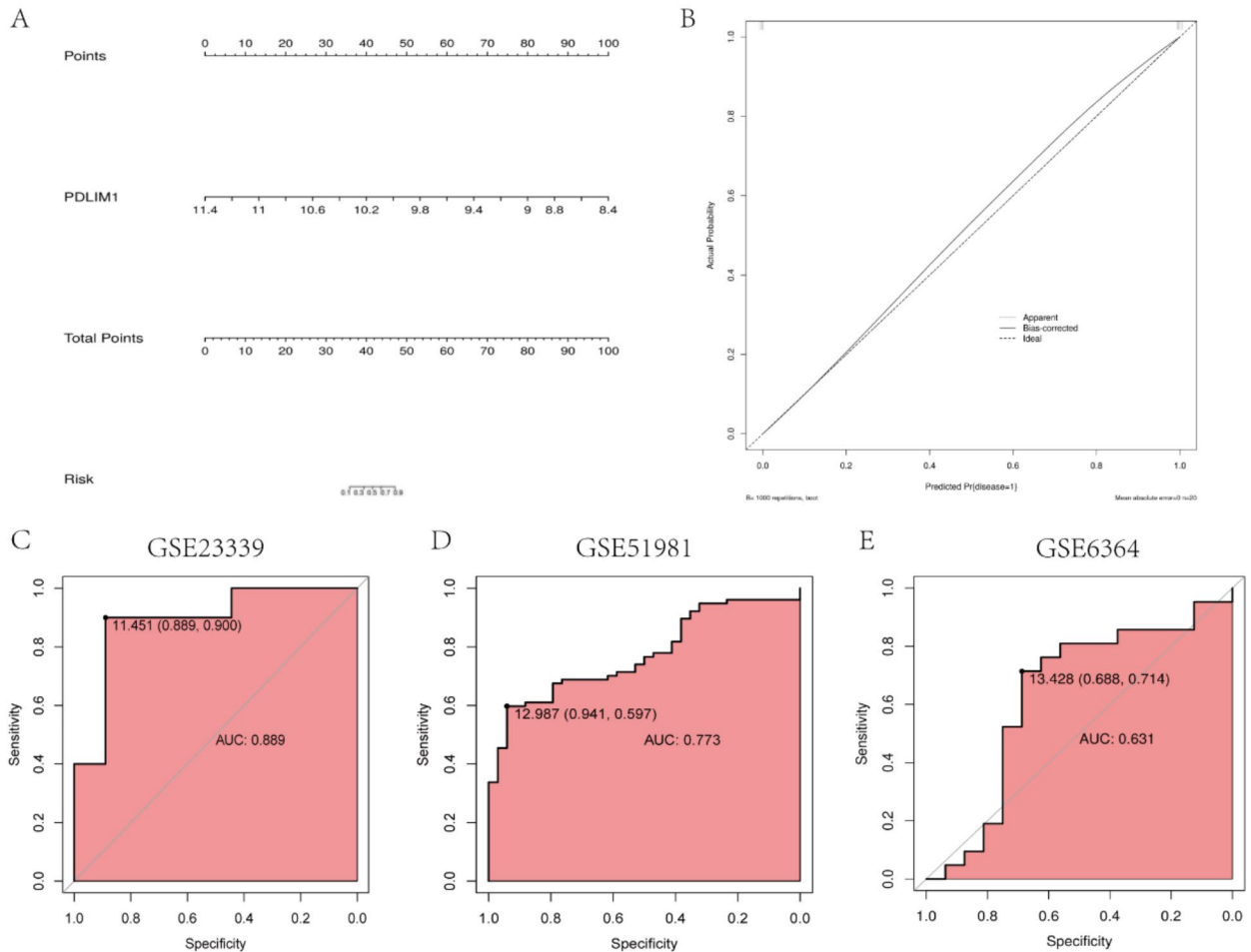
Fig. 6. Diagnostic significance validated using hub genes. (**A**) A nomogram constructed for predicting EMs with hub gene. (**B**) Calibration curve plotted for evaluating the nomogram prediction value. (**C**–**E**) ROC curves of GSE23339, GSE51981, and GSE6364.

In our study, gene expression in EMs and healthy samples was explored using the GEO database. GO and KEGG analyses on differential genes from GSE7305 showed that the cells were mostly associated with the immune receptor activity, positive regulation of Glycosaminoglycan binding, extracellular matrix structural constituent, transcription coactivator activity, Cell adhesion molecules, Cell cycle, Glutathione metabolism, IL-17 pathway, Human T-cell leukemia virus 1 infection, Human T-cell leukemia virus 1 infection, Estrogen pathway, Cytokine-cytokine receptor interaction, Inflammatory bowel disease, Cholesterol metabolism, actin binding and so on. These findings indicate that the immune microenvironment in patients with EMs significantly deviates from that of healthy individuals. In addition, we conducted further analysis of the dataset using GSEA, which revealed that patients with EMs exhibited enhanced humoral immunity, particularly in relation to B-cell receptor-related pathways. Our study suggested aberrant glucose metabolism in patients with EMs, prompting us to postulate a potential association between EMs and disulfidoptosis. Based on the obtained results, we proceeded to investigate DRGs of EMs.

Subsequently, 15 DRGs associated with EMs were found by selecting EMs DEGs and 31 known disulfidptosis genes. The 15 key genes are OXSM, MYH10, RAC1, RPN1, IQGAP1, CD2AP, PDLIM1, GYS1, ACTN4, FLNB, TLN1, PSMD2, CYFIP1, WASF2, and ABI2. Immune cell infiltration analysis was performed, showing significant changes in immune cell populations between normal individuals and those with EMs. Notably, NK cells exhibited the most significant changes, consistent with previous studies[39]. Moreover, they were also significant differences in B cells naive, which was also in consistence with GSEA analysis. Through correlation analysis of 15 hub genes with immune cells, it can be observed that these key genes have a significant relationship to NK cells. These results suggest that differences in EMs immune cells are probably to be closely associated with the regulation of disulfidoptosis.

To further identify hub genes with significant predictive effects among key genes, five machine learning algorithms were used. Finally, PDLIM1 was identified as the hub gene. The prediction effect was significantly improved by incorporating three external datasets for verification. PDLIM1 is an actinin-associated LIM protein (ALP) subfamily member of PDZ-LIM protein family[40]. Also referred to as CLP36, Elfin or CLIM1, PDLIM1
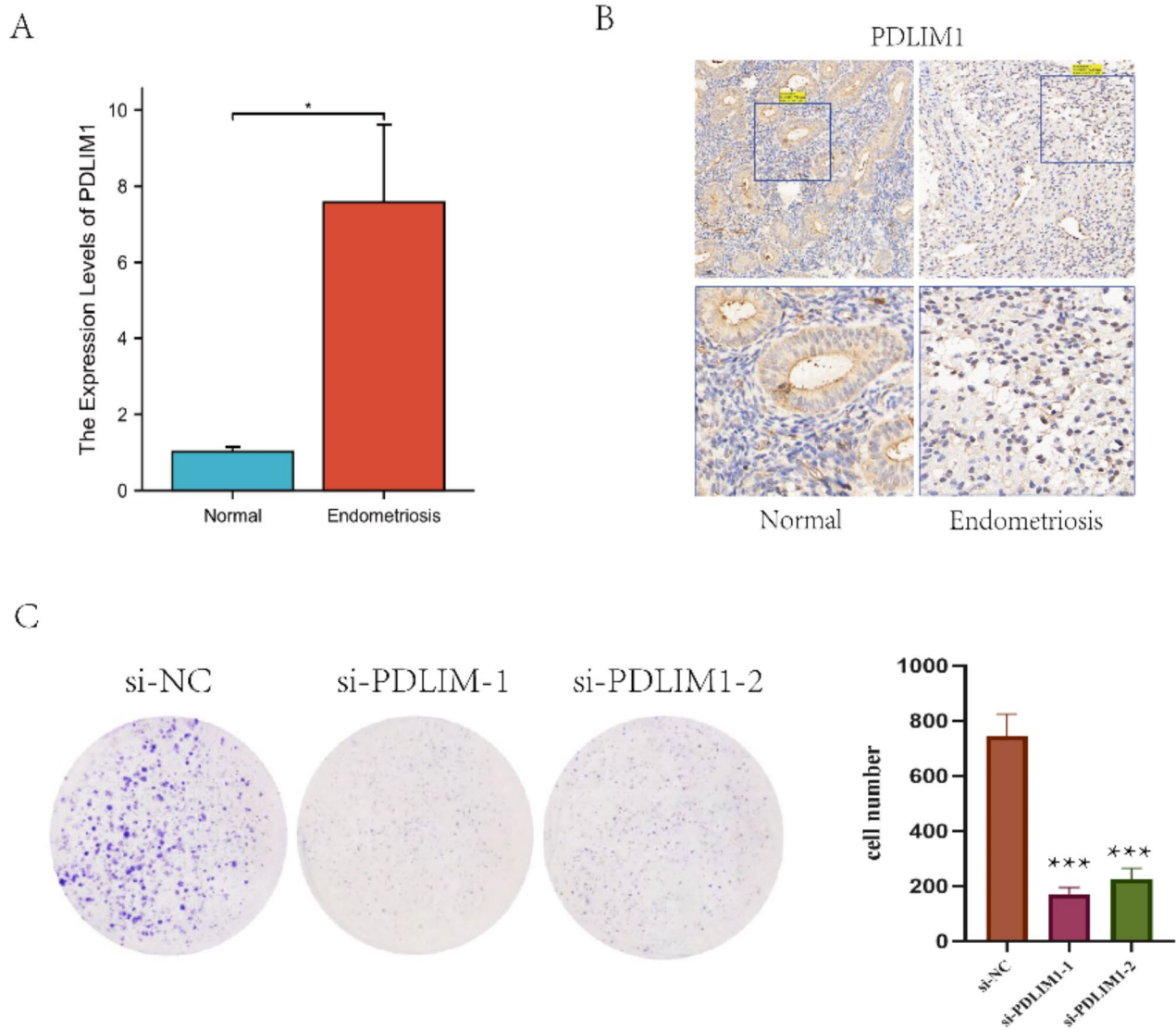
Fig. 7. Results of RT-qPCR and IHC. (**A**) The results of RT-qPCR illustrated PDLIM1 expression in EMs tissues ($n = 3$) and healthy endometrium ($n = 3$). *$p < 0.05$. (**B**) IHC analysis revealed PDLIM1 expression in EMs tissues and normal endometrium. (**C**) The Colony formation assay to determine the effect of PDLIM1 knockdown on the proliferation of EMs primary cells.

makes a vital impact on cytoskeleton organization, neuronal signaling, and organ development by interaction with a variety of proteins like paladin, α-actinin, EGFR and FHL1[41]. PDLIM1 exhibits the wide distribution in cardiac, pulmonary, hepatic, and splenic tissues. Through its interactions with diverse proteins in distinct tissue types, PDLIM1 is actively involved in the regulation of diverse signaling pathways while demonstrating tissue-specific functionalities. PDLIM1 is the cytoskeleton-related protein that exerts a crucial role in governing actin cytoskeleton organization.

PDLIM1 is related to EMT in different cancers. It has shown significant tissue-specific effects in cancer. In addition, it is found to suppress CRC[42] and HCC[43] metastasis, as well as enhance breast cancer[43], CML[44] and other cancer occurrence. Currently, PDLIM1 has been poorly investigated in gynecological diseases, with only one study in ovarian cancer, which shows that for OC patients, their response to anti-PDLIM1 autoantibody exhibit a positive relation to PDLIM1 up-regulation in OC samples. This reveals that anti-PDLIM1 autoantibody can serve as the complementary measure for CA125, which can thereby improve OC detection power. However, studies in EMs are lacking at present. Although our prediction model suggests that PDLIM1 demonstrates a relatively robust diagnostic efficacy, this study also utilized immunohistochemistry for the evaluation of PDLIM1 protein expression, demonstration significant differences between endometrial malignancies and normal endometrial tissues. Moreover, we showed through cell experiments that after PDLIM1 knockdown, the proliferation ability of primary EMs cells decreased significantly. However, due to the limited sample size, it is necessary to perform further comprehensive investigations. In addition, the mechanism of PDLIM1 affecting

EMs through disulfidoptosis still needs to be further explored, which is also our further research direction. Furthermore, our study emphasizes the potential correlation between the immune microenvironment of EMs and disulfidoptosis, suggesting that the investigation of PDLIM1 in the context of endoheterogeneity immunity could open up new avenues for understanding the pathogenesis and progression of EMs.

At the forefront of biomedical research, ML (Machine Learning) and deep learning(DL) algorithms, with their remarkable capabilities, have the potential to help doctors predict individualized treatment options for specific patients. Traditional ML methods are prone to overfitting, especially when dealing with high-dimensional omics data. This led to an understanding that the complexity of the model should be carefully managed to prevent such overfitting. However, recent theoretical advances are challenging this view, especially in the field of DL. Specifically, DL algorithm has inherent regularization characteristics in the process of backpropagation learning. Interestingly, these features actually reduce the risk of overfitting as the network scales, and contrary to what one might expect, adding more nodes or layers can make the model more robust[45–47]. While paying attention to this important problem, our team will make further efforts to develop more advanced algorithms.

Conclusion

To conclude, this study shows that DRGs are correlated with infiltrating immune cells in EMs. In addition, we have identified PDLIM1 as a unique gene related to disulfidoptosis. These findings hold significant potential for enhancing diagnostic assessments of EMs. Furthermore, our research reveals an unprecedented correlation between disulfidoptosis and EM development while suggesting a possible relationship to immunity. Therefore, it provies fresh perspectives on the underlying pathological mechanisms involved and proposes novel avenues for therapeutic approaches targeting EMs.

Data availability

The data are available at https://www.ncbi.nlm.nih.gov/geo/query/acc.cgi? acc=GSE7305, https://www.ncbi.nlm.nih.gov/geo/query/acc.cgi? acc=GSE51981，https://www.ncbi.nlm.nih.gov/geo/query/acc.cgi? acc=GSE23339，https://www.ncbi.nlm.nih.gov/geo/query/acc.cgi? acc=GSE6364，The accession numbers: GSE7305, GSE51981, GSE6364, and GSE51981.

References

1. Bulun, S. E. et al. Endometriosis. *Endocr. Rev.* **40**, 1048–1079 (2019).
2. Burney, R. O. & Giudice, L. C. Pathogenesis and pathophysiology of endometriosis. *Fertil. Steril.* **98**, 511–519 (2012).
3. Taylor, H. S., Kotlyar, A. M. & Flores, V. A. Endometriosis is a chronic systemic disease: clinical challenges and novel innovations. *Lancet* **397**, 839–852 (2021).
4. Othman Eel, D. et al. Serum cytokines as biomarkers for nonsurgical prediction of endometriosis. *Eur. J. Obstet. Gynecol. Reprod. Biol.* **137**, 240–246 (2008).
5. Shigesi, N. et al. The association between endometriosis and autoimmune diseases: a systematic review and meta-analysis. *Hum. Reprod. Update* **25**, 486–503 (2019).
6. Vallvé-Juanico, J., Houshdaran, S. & Giudice, L. C. The endometrial immune environment of women with endometriosis. *Hum. Reprod. Update* **25**, 564–591 (2019).
7. Kyama, C. M., Debrock, S., Mwenda, J. M. & D'Hooghe, T. M. Potential involvement of the immune system in the development of endometriosis. *Reprod. Biol. Endocrinol.* **1**, 123 (2003).
8. Hassa, H., Tanir, H. M., Tekin, B., Kirilmaz, S. D. & Sahin Mutlu, F. Cytokine and immune cell levels in peritoneal fluid and peripheral blood of women with early- and late-staged endometriosis. *Arch. Gynecol. Obstet.* **279**, 891–895 (2009).
9. Reis, F. M., Petraglia, F. & Taylor, R. N. Endometriosis: hormone regulation and clinical consequences of chemotaxis and apoptosis. *Hum. Reprod. Update* **19**, 406–418 (2013).
10. Li, Y., et al. Double-edged roles of ferroptosis in endometriosis and endometriosis-related infertility. *Cell. Death Discov.* **9**, 306 (2023).
11. Lu, J. et al. FDX1 enhances endometriosis cell cuproptosis via G6PD-mediated redox homeostasis. *Apoptosis* **28**, 1128–1140 (2023).
12. Liu, X. et al. Actin cytoskeleton vulnerability to disulfide stress mediates disulfidptosis. *Nat. Cell Biol.* **25**, 404–414 (2023).
13. Wu, Q. et al. Macrophages originated IL-33/ST2 inhibits ferroptosis in endometriosis via the ATF3/SLC7A11 axis. *Cell. Death Dis.* **14**, 668 (2023).
14. Chen, J. P. et al. Effects of dysregulated glucose metabolism on the occurrence and ART outcome of endometriosis. *Eur. J. Med. Res.* **28**, 305 (2023).
15. Hever, A. et al. Human endometriosis is associated with plasma cells and overexpression of B lymphocyte stimulator. *Proc. Natl. Acad. Sci. USA* **104**, 12451–12456 (2007).
16. Hawkins, S. M. et al. Functional microRNA involved in endometriosis. *Mol. Endocrinol. (Baltimore Md)* **25**, 821–832 (2011).
17. Burney, R. O. et al. Gene expression analysis of endometrium reveals progesterone resistance and candidate susceptibility genes in women with endometriosis. *Endocrinology* **148**, 3814–3826 (2007).
18. Tamaresis, J. S. et al. Molecular classification of endometriosis and disease stage using high-dimensional genomic data. *Endocrinology* **155**, 4986–4999 (2014).
19. Ritchie, M. E. et al. Limma powers differential expression analyses for RNA-sequencing and microarray studies. *Nucleic Acids Res.* **43**, e47 (2015).
20. Yu, G., Wang, L. G., Han, Y. & He, Q. Y. clusterProfiler: an R package for comparing biological themes among gene clusters. *Omics: J. Integr. Biol.* **16**, 284–287 (2012).
21. Zheng, P., Zhou, C., Ding, Y. & Duan, S. Disulfidptosis: a new target for metabolic cancer therapy. *J. Exp. Clin. Cancer Res.* **42**, 103 (2023).
22. Chen, B., Khodadoust, M. S., Liu, C. L., Newman, A. M. & Alizadeh, A. A. Profiling tumor infiltrating immune cells with CIBERSORT. *Methods Mol. Biol. (Clifton, NJ)* **1711**, 243–259 (2018).
23. Hänzelmann, S., Castelo, R. & Guinney, J. GSVA: gene set variation analysis for microarray and RNA-seq data. *BMC Bioinform.* **14**, 7 (2013).

24. Gustavsson, E. K., Zhang, D., Reynolds, R. H., Garcia-Ruiz, S. & Ryten, M. Ggtranscript: an R package for the visualization and interpretation of transcript isoforms using ggplot2. *Bioinformatics (Oxford England)* **38**, 3844–3846 (2022).
25. Huang, L., Wu, C., Xu, D., Cui, Y. & Tang, J. Screening of important factors in the early sepsis stage based on the evaluation of ssGSEA algorithm and ceRNA regulatory network. *Evol. Bioinf. Online* **17**, 11769343211058463 (2021).
26. Kang, J. et al. LASSO-based machine learning algorithm for prediction of lymph node metastasis in T1 colorectal cancer. *Cancer Res. Treat.* **53**, 773–783 (2021).
27. Zhao, Z. et al. Analysis and experimental validation of rheumatoid arthritis innate immunity gene CYFIP2 and pan-cancer. *Front. Immunol.* **13**, 954848 (2022).
28. Wei, W., Li, Y. & Huang, T. Using machine learning methods to study colorectal cancer tumor micro-environment and its biomarkers. *Int. J. Mol. Sci.* **24**,13 (2023).
29. Shin, H. XGBoost regression of the most significant photoplethysmogram features for assessing vascular aging. *IEEE J. Biomed. Health Inf.* **26**, 3354–3361 (2022).
30. Zhang, Y. et al. Down-regulation of exosomal Mir-214-3p targeting CCN2 contributes to endometriosis fibrosis and the role of exosomes in the horizontal transfer of miR-214-3p. *Reprod. Sci.* **28**, 715–727 (2021).
31. Vercellini, P., Viganò, P., Somigliana, E. & Fedele, L. Endometriosis: pathogenesis and treatment. *Nat. Rev. Endocrinol.* **10**, 261–275 (2014).
32. Chen, H., Yang, W., Li, Y., Ma, L. & Ji, Z. Leveraging a disulfidptosis-based signature to improve the survival and drug sensitivity of bladder cancer patients. *Front. Immunol.* **14**, 1198878 (2023).
33. Xiong, R. et al. Ferroptosis: a new promising target for lung cancer therapy. *Oxid. Med. Cell Longev.* **2021**, 8457521 (2021).
34. Wang, Y. et al. Nanoparticle-mediated convection-enhanced delivery of a DNA intercalator to gliomas circumvents temozolomide resistance. *Nat. Biomed. Eng.* **5**, 1048–1058 (2021).
35. Wang, X. et al. Disulfidptosis: six riddles Necessitating solutions. *Int. J. Biol. Sci.* **20**, 1042–1044 (2024).
36. Zhang, C. et al. Development and experimental validation of a machine learning-based disulfidptosis-related ferroptosis score for hepatocellular carcinoma. *Apoptosis* **29**, 103–120 (2024).
37. Ma, S., Wang, D. & Xie, D. Identification of disulfidptosis-related genes and subgroups in Alzheimer's disease. *Front. Aging Neurosci.* **15**, 1236490 (2023).
38. He, D. et al. Elaboration and validation of a prognostic signature associated with disulfidoptosis in lung adenocarcinoma, consolidated with integration of single-cell RNA sequencing and bulk RNA sequencing techniques. *Front. Immunol.* **14**, 1278496 (2023).
39. Jiang, H. et al. Bioinformatics identification and validation of biomarkers and infiltrating immune cells in endometriosis. *Front. Immunol.* **13**, 944683 (2022).
40. Zheng, M., Cheng, H., Banerjee, I. & Chen, J. ALP/Enigma PDZ-LIM domain proteins in the heart. *J. Mol. Cell Biol.* **2**, 96–102 (2010).
41. Zhou, J. K., Fan, X., Cheng, J., Liu, W. & Peng, Y. PDLIM1: structure, function and implication in cancer. *Cell Stress*. **5**, 119–127 (2021).
42. Chen, H. N. et al. PDLIM1 stabilizes the E-cadherin/β-catenin complex to prevent epithelial-mesenchymal transition and metastatic potential of colorectal cancer cells. *Cancer Res.* **76**, 1122–1134 (2016).
43. Huang, Z. et al. PDLIM1 inhibits tumor metastasis through activating hippo signaling in hepatocellular carcinoma. *Hepatology* **71**, 1643–1659 (2020).
44. Li, L. M., Luo, F. J. & Song, X. MicroRNA-370-3p inhibits cell proliferation and induces chronic myelogenous leukaemia cell apoptosis by suppressing PDLIM1/Wnt/β-catenin signaling. *Neoplasma* **67**, 509–518 (2020).
45. Sharma, A., Lysenko, A., Jia, S., Boroevich, K. A. & Tsunoda, T. Advances in AI and machine learning for predictive medicine. *J. Hum. Genet.* **69**, 487–497 (2024).
46. Goecks, J., Jalili, V., Heiser, L. M. & Gray, J. W. How machine learning will transform biomedicine. *Cell* **181**, 92–101. (2020).
47. Petzschner, F. H. Practical challenges for precision medicine. *Science* **383**, 149–150 (2024).

Acknowledgements

Author contributions

Writing-manuscript drafting, C; writing-review and editing, M. The authors agreed to the final version for submission.

Funding

Declarations

Competing interests

The authors declare no competing interests.

Ethics statement

Human studies gained approval (ID 2023-KY-030-01) from the Medical Ethics Committee affiliated to Beijing Obstetrics and Gynecology Hospital, Beijing Maternal and Child Health Care Hospital. Informed consents were obtained from all participants prior to participation in the work.

Additional information

Correspondence and requests for materials should be addressed to J.M.

Reprints and permissions information is available at www.nature.com/reprints.

Publisher's note Springer Nature remains neutral with regard to jurisdictional claims in published maps and institutional affiliations.